Iraqi Laser Scientists Journal (ILSJ)/ www.ilsj-online.org
Vol .1, Issue 2; Pp;22-35, 2018.

Original article

Effect of laser wavelength on liver tissue thermal damage in laser induced interstitial thermotherapy

Khalid Salem Shibib, Mohammed A. Munshid, Hind Ali Lateef
Department of Laser and Optoelectronic Engineering, University of Technology, Baghdad, Iraq

Abstract

In the current work, the finite element method (FEM) has been used to predict the damage zone in tissue subjected to laser in laser induced interstitial thermotherapy(LITT). The effect of laser wavelength on thermal damage zone in this technique has been predicted using FEM. It is found that at 850 nm laser wavelength, the damage zone reached its maximum value comparing with other wavelengths. A computer program written in Visual Basic language has been created to solve the problem following FEM procedure. The created program has been verified by comparing its result with that published elsewhere. The simulation depends on bio-heat equation together with liner laser source which was used to simulate heat transfer through tissue depending on its optical and thermal properties where the temperature distribution is obtained from which one can predict the damage zone based on Arrhenius equation assume optical and thermal tissue properties are function of temperature and an iteration solution was carried out to successfully model their variation and their effect on the result. **Key words:** LITT, Thermal damage, LASER

To cite this article: Khalid Salem Shibib, Mohammed A. Munshid & Hind Ali Lateef ; Effect of laser wavelength on liver tissue thermal damage in laser induced interstitial thermotherapy; Iraqi Laser Scientists Journal. Vol .1, Issue 2; Pp;22-35, 2018.

Introduction:

Laser was used in a wide range in medical application such as surgery, gynecology, urology, dermatology, cardiology, ophthalmology and gastrointestinal etc.,(1). Laser-induced interstitial thermotherapy is the technique for tumor treatment by coagulating tissue depends on the transformation of the light that absorbed by the tissue into heat. Optical fiber is used to transmit light, which is inserted deep into the tumor mass. This treatment can be used in different kinds of tumor such as liver, brain, retina, prostate, and uterus ,(1&2). The light source of LITT process is an Nd: YAG laser (1064nm) or diode laser at the wavelength (800-980 nm) which deeply penetrates into biological tissue in the range of near infrared , (3). Ordinarily LITT process is accomplished using diffusing laser applicator which is put into the tumor, as shown in figure ;1

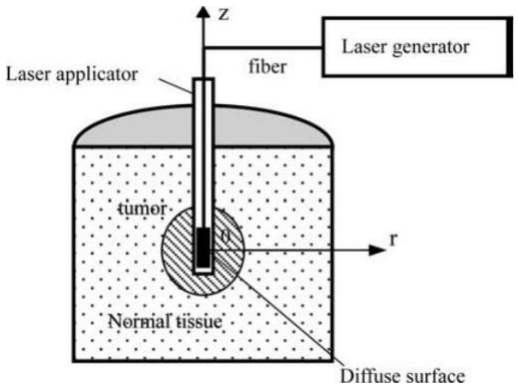

Figure; 1: Schematic diagram of LITT for treating a tumor in biological tissues

Jiang, S. C. et.al. , (4) ,studied the effects of dynamic changes optical properties, thermal properties, and blood perfusion on tissue temperature and damage to simulate LITT for human liver using two-dimensional model. Salavati , et.al. , (5) ,used FEM to solve bio-heat equation and Arrhenius equations to obtain distribution of temperature and thermal damage in liver human tissue using laser at 850 nm. Chapman, R., (6) ,studied LITT treatment of uterine leiomyomas using (KTP/YAG) laser at wavelength 532 nm and 1064 nm respectively and diode laser at wavelength 810 nm. Zhang, H. et al., (7), used Monte Carlo method to simulate propagations of NIR laser in liver tumor to study the effect of laser power and action time on temperature distribution using laser at 808 nm. Saccomandi , et. al.,(8), studied theoretically the thermal response of human pancreatic tissue treated by laser-induced interstitial thermotherapy using an Nd: YAG laser at wavelength of 1064 nm at different powers.

In the current work, FEM was used to predict temperature distribution and thermal damage volume of human liver treatment using three laser wavelengths (850, 980 and 1064nm) and it was found that the laser at wavelength of 850 nm gives the greatest thermal damage volume in liver tissue.

Theory:

1.Bio-heat equation:

The bio-heat equation depends on the classical Fourier theory of heat conduction and is utilized for modeling the heating in biological tissue, (9&10). The model depends on the energy exchange between the blood vessels and surrounding tissues , (11) ,then the bio-heat equation can be written as:

$$\rho c \frac{\partial T}{\partial t} = \nabla .(k \nabla T) + \rho_b c_b \omega_b (T_b - T) + Q_m + Q_r \qquad (1)$$

Where ρ is the density of tissue [kg.cm^{-3}], c is the specific heat of tissue [J.kg^{-1}.^{o}C^{-1}], k is thermal conductivity of tissue [W.m^{-1}.^{o}C^{-1}], T is the tissue temperature [˚C], t is the time [s], ρ_b blood density [kg.m^{-3}], c_b specific heat of blood [J.kg^{-1}.C$^{\circ -1}$], ω_b blood perfusion rate per unit volume [m^{3}.m^{-3}.s^{-1}], T_b is the arterial blood temperature which is normally assumed to be fixed

at 37 ˚C, Q_r is internal heat source term due to photon absorption [W.m^{-3}], and $Q_m$is the metabolic heat generation per unit volume which is usually negligible comparing with heat produced from laser absorption[4,6]. An easily transform procedure from Cartesian to axis symmetry region domain is followed since the region of interest has an axis symmetry form, (12).

2. laser heat source:

The internal heat source due to photon absorption could be given by [8]:

$$Q_r = \mu_a \emptyset(r) \qquad (2)$$

Where $\emptyset(r)$ is fluence rate [W/m^2] and μ_a is absorption coefficient (m^{-1}). The simplest method to get the fluence rate at a certain distance from a linear light source is to approximate this source by a chain of n discrete isotropic point sources with power P, Let the linear source have length and be position on the z-axis with the center at z = 0 as shown in figure; 2, then the fluence rate at point r can be given by ,(13).

$$\emptyset(r) = \frac{3P^{*}\mu_{tr}\exp(-\mu_{eff}r)}{\sqrt{8\pi}\sqrt{\mu_{eff}r}}\left[1 - 1/(8\mu_{eff}r)\right] \qquad (3)$$

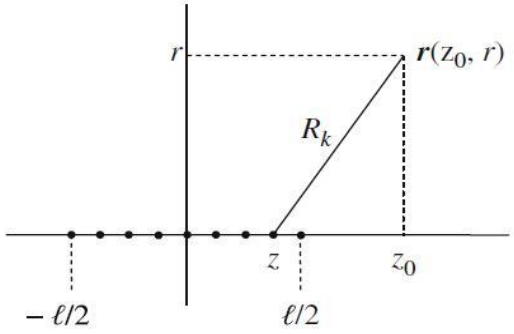

Figure;2: The geometry for the calculation of the fluence rate in tissue due to a linear light source simulated by point sources (black dots)

where μ_{tr} is transport attenuation coefficient [m^{-1}] and μ_{eff} is effective attenuation coefficient [m^{-1}].

$$P* = nP/ \text{ [W/m]} \qquad (4)$$

$$\mu_{tr} = \mu_a + \mu_s(1-g) \qquad (5)$$

$$\mu_{eff} = \sqrt{3\mu_a\mu_{tr}} \qquad (6)$$

μ_a is absorption coefficient [m^{-1}], μ_s is scattering coefficient [m^{-1}] and g is Anisotropy factor.

It is clear now that the absorbed heat in tissue depends mainly on optical and thermal tissue properties, see eqs. ,(2- 6).

3. Arrhenius equation:

Thermal damage in normal tissue and tumor can be predicted mathematically by Arrhenius equation where damage is quantified by utilizing a single parameter Ω [14,15]:

$$\Omega(r,\tau) = A_f \int_0^{\tau} \exp\left(\frac{-E_a}{RT(r,\tau)}\right) dt \qquad (7)$$

Where; τ is time(s), A_f frequency factor = $9.4*10^{104}$ s^{-1} for liver, E_a activation energy = $6.68*10^{5}$ J mol^{-1} for liver, R universal gas constant= 8.31 J $mol^{-1}K^{-1}$, and T (K) is the temperature, (4&15) ,Ω=1 is referred to the denaturation state of about 63% of volume, which indicate irreversible tissue damage and the changing of the optical properties from the native to the coagulated value, (16). When tissue temperatures reach 60 to 65 ^{o}C tissue damage can be expectant, evaporation and even carbonization will occur if the tissue temperature increased above 100 ^{o}C which should be avoided during LITT ,(3 &17) .The undamaged fraction of the tissue can be found by $f_u = \exp(-\Omega)$, while the damaged fraction is $f_d = (1 - f_u)$,(18).

4. Optical and thermal properties of tissue:

Heat and thermal damage caused changes in the optical properties of tissue, and these changes effect the temperature distribution during laser irradiation. The optical properties of tissue are given by , (2&3);

$$\mu_a = \mu_{a,native} f_u + \mu_{a,coag} f_d \qquad (8)$$

$$\mu_s = \mu_{s,native} f_u + \mu_{s,coag} f_d \qquad (9)$$

$$g = g_{native} f_u + g_{coag} f_d \qquad (10)$$

The native and coagulated optical properties for human liver tissues are shown in tables 1-3

Table (1): Optical properties at 850nm for normal and tumor human liver tissue before and after coagulation, (4).

Tissue type	μ_a (mm^{-1})	μ_a (mm^{-1})	g
Native normal liver tissue	0.10	20.4	0.995
Coagulated normal liver tissue	0.07	23.6	0.887
Native liver tumor	0.06	10.8	0.902
Coagulated liver tumor	0.05	10.4	0.827

Table (2): Optical properties at 980nm for normal and tumor human liver tissue before and after coagulation, (4).

Tissue type	μ_a (mm^{-1})	μ_a (mm^{-1})	g
Native normal liver tissue	0.08	18.2	0.955
Coagulated normal liver tissue	0.05	21.0	0.896
Native liver tumor	0.06	11.3	0.914
Coagulated liver tumor	0.05	10.5	0.860

Table (3): Optical properties at 1064nm for normal and tumor human liver tissue before and after coagulation, (4).

Tissue type	μ_a (mm^{-1})	μ_a (mm^{-1})	g
Native normal liver tissue	0.05	16.9	0.952
Coagulated normal liver tissue	0.02	20.0	0.904
Native liver tumor	0.03	10.9	0.917
Coagulated liver tumor	0.02	10.3	0.865

Thermal properties of tissue can be approximated according to their water content and the dynamic change of thermal properties of water in range 20–100^{o}C are,(3).

$$\rho(T) = 1{,}000\left(1.3 - 0.3k_{\rho}w\right) \quad kgm^{-3} \qquad (11)$$

$$c(T) = 4{,}190(0.37 + 0.63k_{c}w) \quad Jkg^{-1}K^{-1} \qquad (12)$$

$$k(T) = 0.419(0.133 + 1.36k_{k}w) \quad Wm^{-1}K^{-1} \qquad (13)$$

Where w is the tissue water content which is about 69% for the liver tissue and T (^{o}C) is tissue temperature. The factors k_{ρ}, k_c and k_k are temperature-dependent for density, specific heat and thermal conductivity of water, respectively,(3).

$$k_{\rho} = 1 - 4.98 * 10^{-4}(T - 20°C) \qquad (14)$$

$$k_{c} = 1 + 1.016 * 10^{-4}(T - 20°C) \qquad (15)$$

$$k_{k} = 1 + 1.78 * 10^{-3}(T - 20^{0}C) \qquad (16)$$

5. Blood perfusion:

The dynamic changes of blood perfusion rate with temperature and damage can be formulated as:

$$\omega_b(T,\Omega) = \omega_{bo} f_T f_u \qquad (17)$$

Where ω_{b0} is the blood perfusion rate= 0.0182 m^3 m^{-3} s^{-1} for liver, f_u is the undamaged fraction of the tissue and f_T is a dimensionless function that accounts for vessel dilation at a little elevated temperatures which can be approximated as [5]:

$$f_T = \begin{cases} 4 + 0.6(T - 42C^o) & 37C^o \le T < 42C^0 \\ 4 & T \ge 42^o C \end{cases} \qquad (18)$$

6. Finite Element Formulation:

The region of interest is divided by a sufficient number of elements that well model the physical domain. The solution of bio-heat equation subject to the special boundary conditions could be accomplished using Galerkin method. The studied region is divided into a number of elements with linear shape function N_i at each node. Unknown function T is approximated through the solution domain at any time by:

$$T = \sum N_i\ (x,t) T_i(t) \qquad (19)$$

Where $T_i(t)$ is the nodal temperature. Substitution of the above equation into bio-heat equation and the application of Galerkin method results in a system of ordinary differential equations ,(19&20).

$$[C]\dot{\vec{T}} + [K]\vec{T} + [F] = 0 \qquad (20)$$

Where:

$$\dot{T} = \begin{Bmatrix} \frac{\partial T_1}{\partial t} \\ \frac{\partial T_2}{\partial t} \\ \vdots \\ \frac{\partial T_p}{\partial t} \end{Bmatrix}, \quad T = \begin{Bmatrix} T_1 \\ T_2 \\ \vdots \\ T_p \end{Bmatrix} \text{ and } [F] = \begin{Bmatrix} F_1 \\ F_2 \\ \vdots \\ F_p \end{Bmatrix} \quad \text{here p is the total no. of nodes} \qquad (21)$$

and the typical matrix elements are

$$K_{ij} = \sum k\left(\frac{\partial N_i}{\partial x}\frac{\partial N_j}{\partial x}\right)dV + \int_{V^e} (N_i N_j f_t f_u \omega_b C_b \rho_b)dV \qquad (22)$$

$$C_{ij} = \sum \int_{V^e} \rho c N_i N_j dV \qquad (23)$$

$$F_i = -\sum \int_{V^e} Q_r\, dV - \int_{V^e} (f_t f_u \omega_b C_b \rho_b T_b)dV \qquad (24)$$

In the above, summation are taken over the contribution of each element, V^e, in the element region and using linear shape function which normalize to time interval. The result is in standard linear shape function, so the application of weighted residual theory to eq.20 with linear shape function, result is in the matrix form of :

$$\left(\frac{[C]}{\Delta t} + \Theta[K]\right)T_{n+1} + \left(\frac{-[C]}{\Delta t} + (1-\Theta)[K]\right)T_n + F = 0 \qquad (25)$$

Where:

$$F = F_{n+1}\,\Theta + F_n\,(1-\Theta) \qquad (26)$$

Θ can has different value. In this solution a forward difference was chosen due to its simplicity (i.e. $\Theta = 0$) and an iteration solution was used at each time step to insure accurate results. It is assumed that all boundary conditions on the outer surfaced region are adiabatic due to the fact that no boundary heat transfer is exist due to symmetry (at z-axis and r- axis) and due to the fairness of outer coordinate from scatter (at the outer surface of the studied region).

The procedure of the solution was as follow: Starting with initially assumed temperature of 37C through the studied region, the pumping of radially diffused laser is started. The nearby tissue will absorb the energy of laser photons causing its temperature to raise changing optical and thermal tissue properties which can be incorporated into the solution by iteration solution. At each time step the new temperature distribution and thermal damage extent were calculated till the solution reach a previously assigned time. (i.e. 40 s , 80 s and 100 s) , as will be shown later.

Results and discussion

Finite element method has been used successfully to solve bio-heat equation where a line heat source is used which is produced from a line laser source (scatterer) which has 10 cm for length and 1 mm in radius. A computer program based on Visual Basic is created following the flow chart shown in fig; 3 :

The axis symmetry studied region, with width of 2 cm and height of 3 cm, is shown in fig 4 , where the region is divided into 605 elements with 329 nodes. A time step of 0.025s is chosen with initial temperature distribution of 37 ^{o}C. A fine mesh was used in the expected intense heat

generation region and coarser mesh elsewhere. To insure accurate result a small time step was chosen to insure stability also an iteration solution was used to well model the problem, assume the thermal and optical tissue properties of tissue were a function of temperature.

At power 5 W and 40 s of treatment. the resulting thermal damage volume of liver tissue at wavelength 850 nm which obtain from the program is compared with that of Jiang ,(4) and a

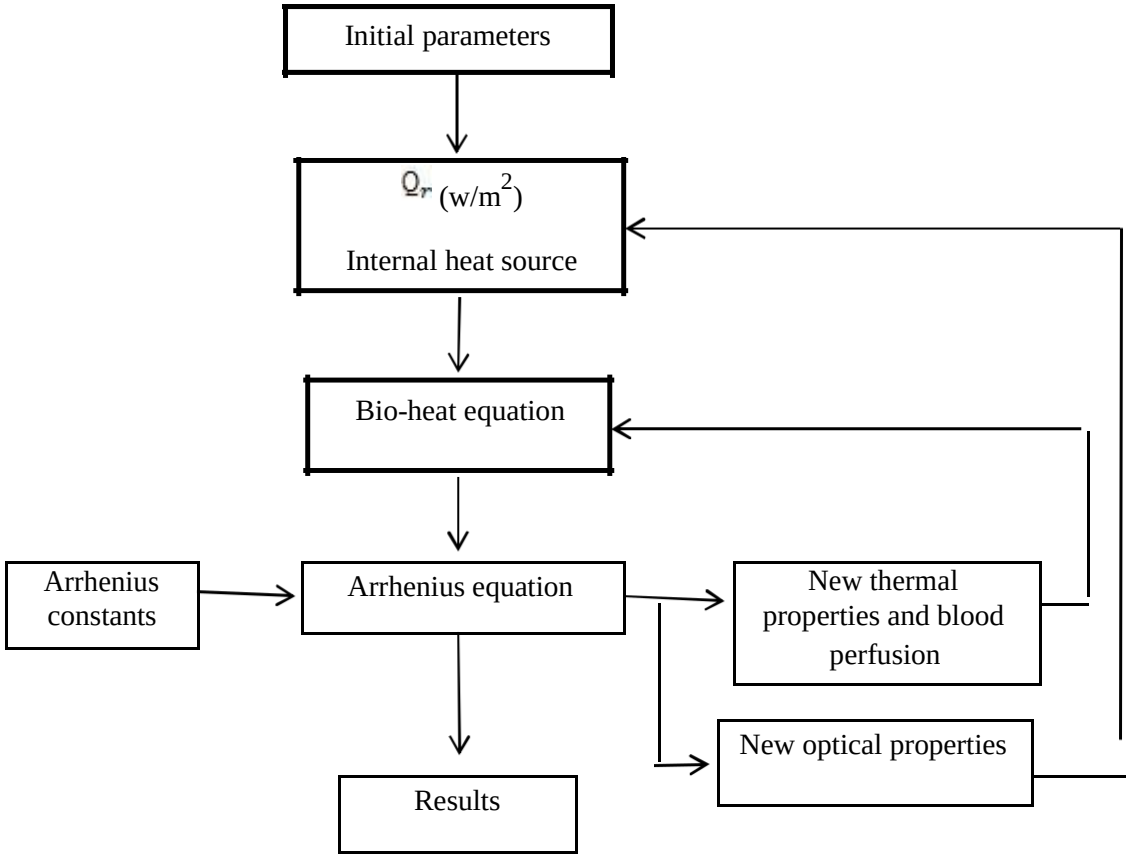

Figure;3 : Flow chat of temperature and damage zone prediction

good nearby result is obtained. The difference between the damage volume obtain from this work and that obtained be reference ,(4) is less than 1%., see fig; 5.

scatterer

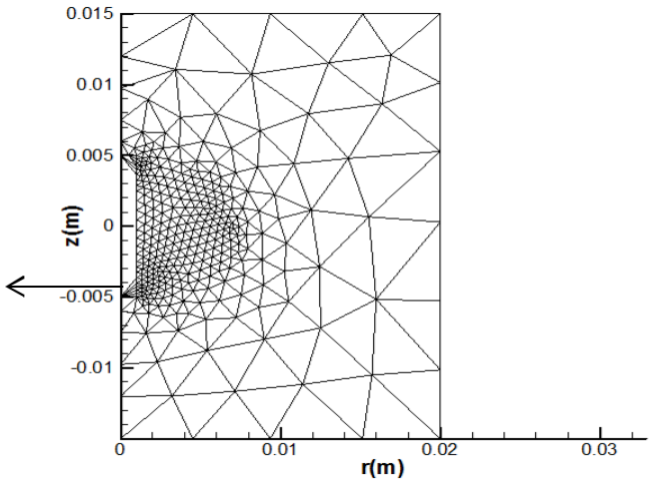

Figure; 4: The discretization of the studied physical domain

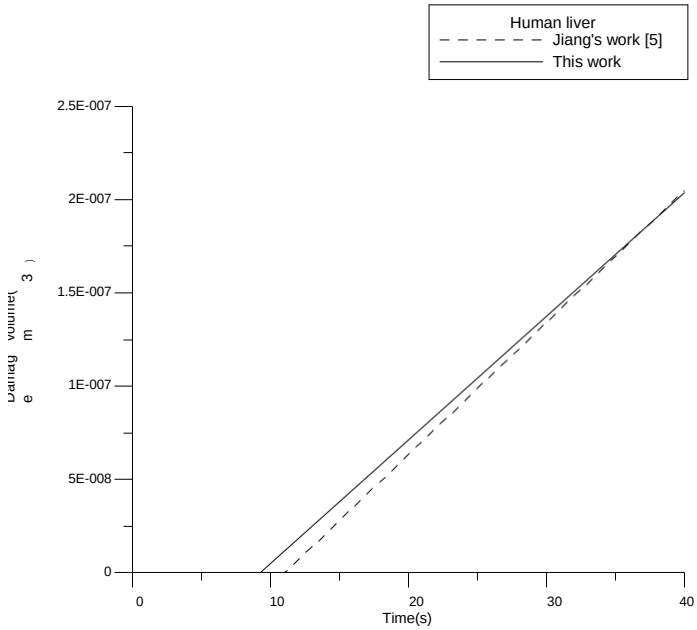

Figure;5: The comparison of thermal damage volume obtained from this work and Jiang's work of human liver tissue at power 5 W and wavelength of 850 nm.

Maximum temperature history that occurred in the human liver tissue at power of 5 W and wavelengths of (850, 980 and 1064nm) are shown in fig 6. It is increased with time and after 80 s of laser radiation, the power was turned off and the temperature is dropped. This drop in temperature is due to the fact that heat was carried out of a high temperature region to a low temperature region by blood perfusion and heat conduction.

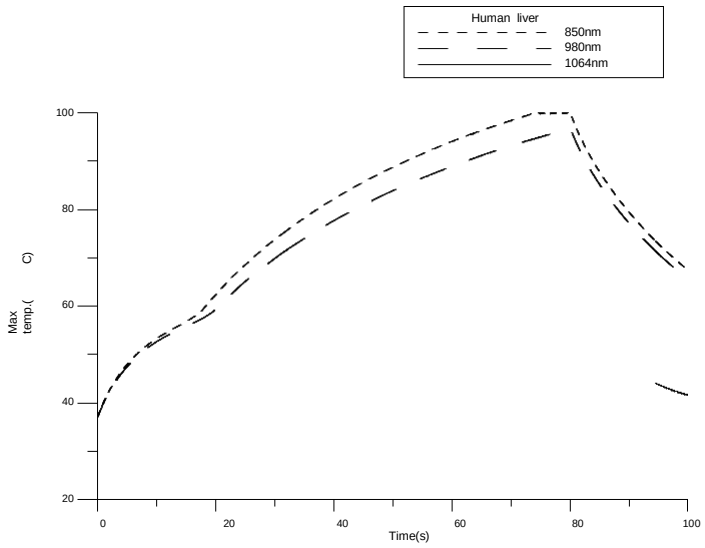

Figure;6: Max temp. in human liver tissue at power of 5 W and wavelengths of 850, 980 and 1064nm.

Thermal damage volume history is shown in fig. 7, which shows that the damage volumes increased with time since more heat will be generated as the laser pumping is on result in increasing damage volume. It is clear that the maximum temperature and maximum thermal damage volume occur at laser wavelength of 850 nm comparing with other wavelengths. This is due to the optical properties of liver where the absorption coefficient of liver recorded its maximum value at that wavelengths ,tables; 1-3 this is result from the increasing in heat generation that cause an increasing in temperature distribution and the subsequent thermal damage. A small increase in the damage volume is observed as the power is turned off after 80 s of treatment, this is due to the fact that the blood will speedily carry the heat away from the hotter region to the relatively cooled region and the damage increase is stopped after the temperatures drop below 60^{o} C where under this temperature damage in tissue can be ignored [1] where the increase in the damage volumes are 1.12%, 3.1% and 12.2% for wavelengths of 850, 980 and 1064 nm, receptively, figure; 7.

The temperature distribution in tissue after 80 s of laser radiations at wavelength 850 nm is shown in fig 8. It is clear that the intense laser radiation near the scatterer cause the observed increase in temperature nearby which is still below 100^{o} C which is avoided as mentioned earlier. The resulting damage zone due to temperature increase is shown in fig 9. It is assumed that the contour of the damaged region is drawn between the finite element nodes that reached the irreversible damage (i.e. Ω=1), see eq. 7.

Figures; 10 and 11 show the temperature distribution and damage zone after 80 s power on then 20 s power off. A significant reduction in temperature distribution is observed due to the fact that the heat will spread out of the hotter region as discussed before also a small increase in the damage volume is observed as the laser pumping is off which is due to reduce in the temperature distribution also this case is studied earlier.

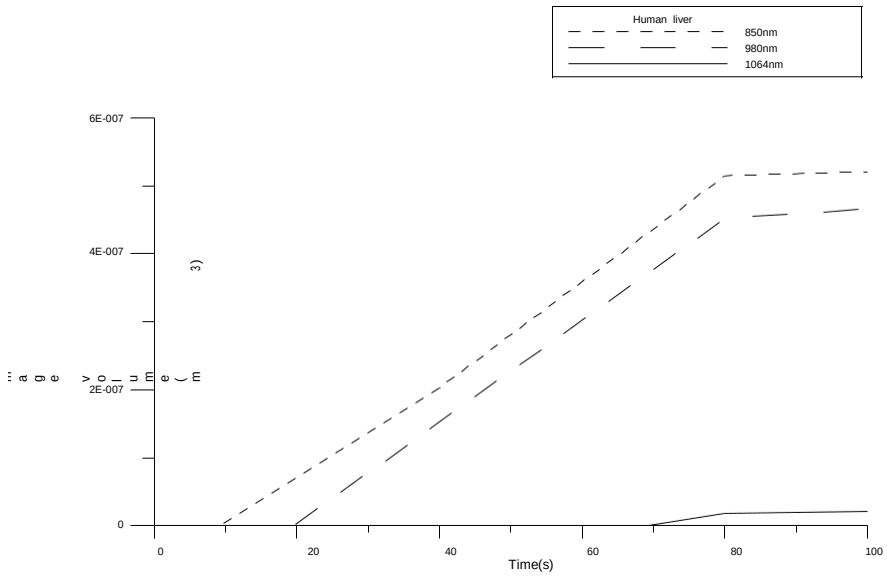

Figure;7: Variation of tissue damage volume with time at power of 5 W and wavelengths of 850,980 and 1064 nm.

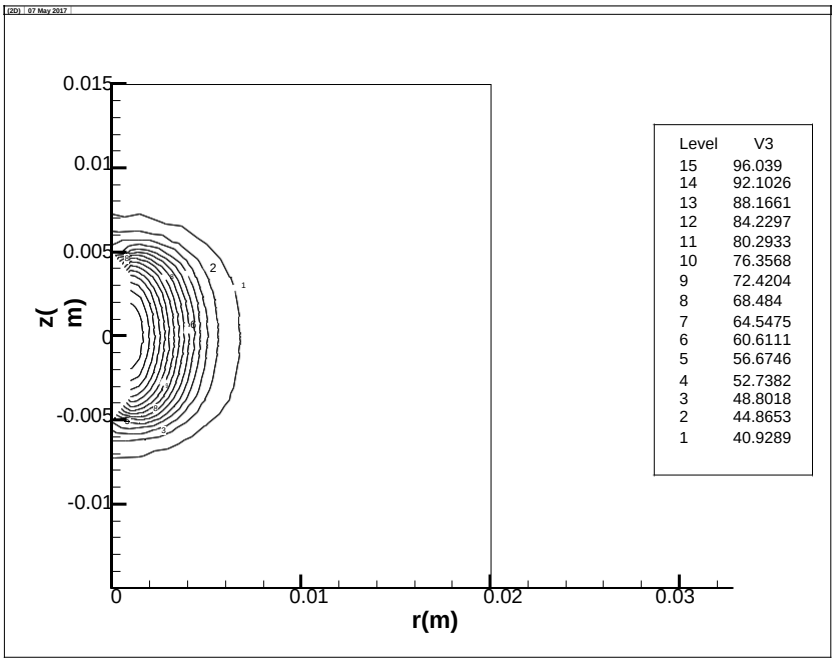

Figure;8 Temperature distribution of tissue at 850 nm after 80 s of 5 W laser power

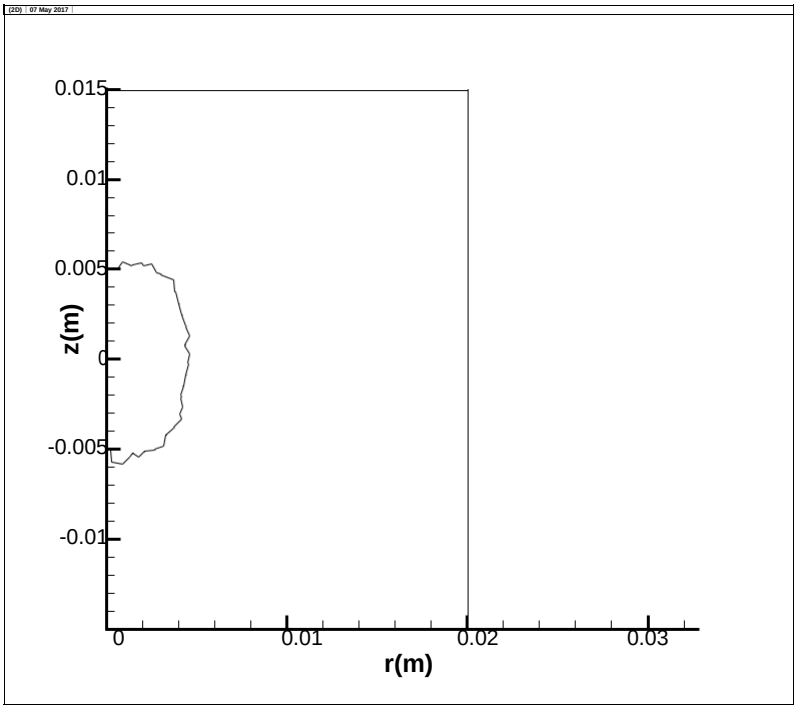

Figure;9: Damage zone of tissue at 850 nm after 80 s of 5W laser power

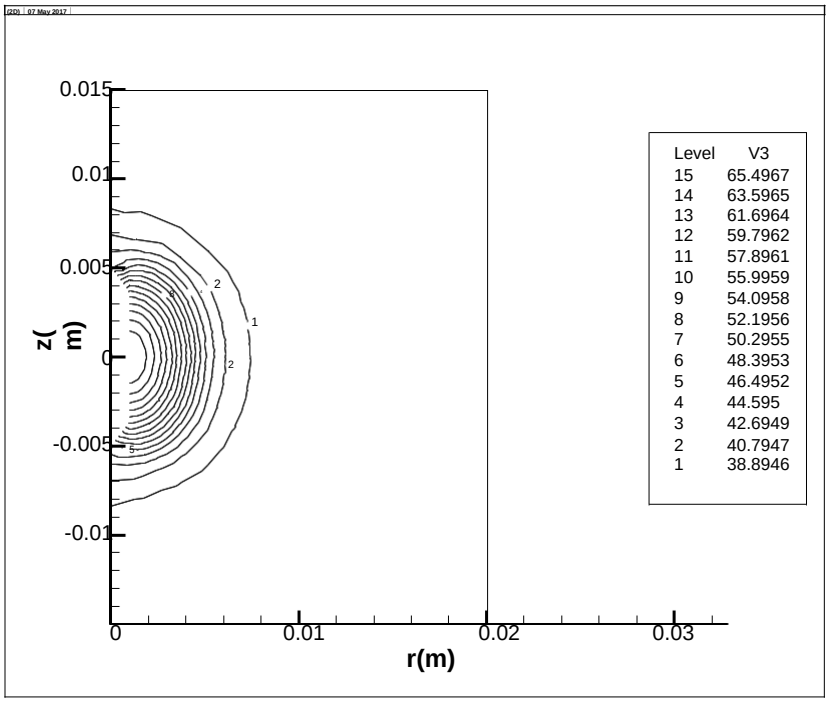

Figure;10: Temperature distribution of tissue at 850nm of 5 W laser power after 100s (80s power on then 20s power off)

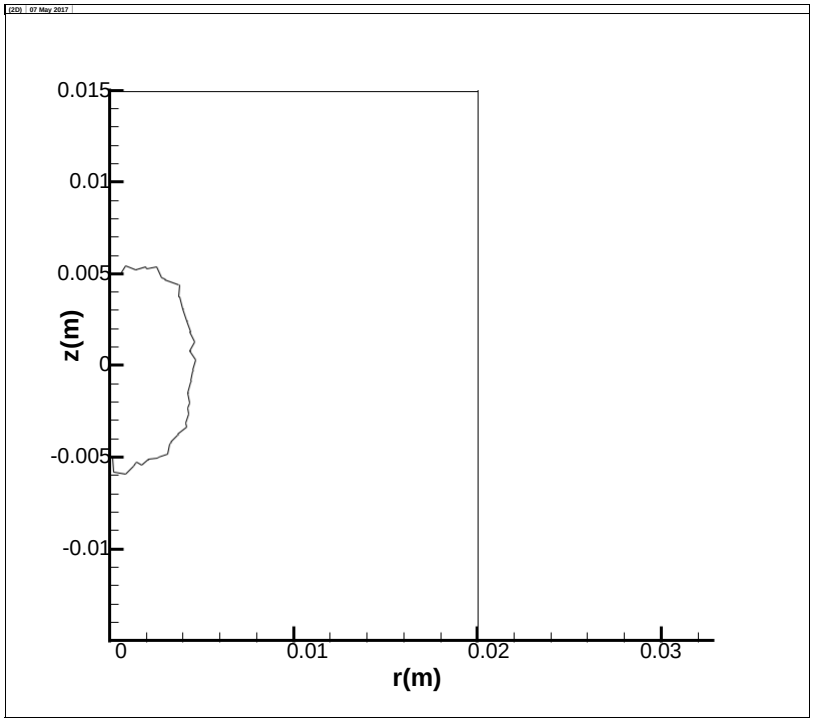

Figure;11: Tissue damage zone at 850nm of 5W laser power after 100 s (80 s power on then 20 s power off)

Conclusions

The finite element method has been used successfully to predict the temperature distribution and damage volume in tissue subjected to linear heat source in LITT technique where laser power is diffused radially causing thermal damage. An axis symmetry bio-heat equation with radially diffused laser was used where the changing blood perfusion, thermal and optical tissue properties through the procedure is incorporate using iterative solution. The results from this work were compared with other published data with good nearby result. Three wavelengths 850, 980 and 1064 nm were tested at laser power of 5 W. It is found that maximum damage was occurs at 850 nm, this is due to the high absorption coefficient of tissue at this wavelength. It is also found that the damage zone is increased with time and stopped after a while after stopping laser pumping which is due to the fact that the temperature nearby still be high enough to cause small damage after that the damage is stopped due to a significant reduction in temperature nearby. Finally, it is worthwhile to know the appropriate laser wavelength that can cause maximum damage in LITT so as to select the most effective laser wave length in LITT procedure.

References

1. Niemz, M. H., Laser-Tissue Interactions: Fundamentals and Applications, Springer Science & Business Media, Berlin, Germany, 2007.
2.Sturesson, C., Medical Laser-Induced Thermotherapy-Models and Applications, Ph. D. thesis, Lund Institute of Technology, Lund, Swed,1998.

3.Jiang, S. C., Zhang, X. X., Dynamic Modeling of Photothermal Interactions for Laser-Induced Interstitial Thermotherapy: Parameter Sensitivity Analysis, *Lasers in Medical Science, 20* (2005), 3, pp. 122-131.
4. Jiang, S. C., Zhang, X. X., Effects of Dynamic Changes of Tissue Properties During Laser-Induced Interstitial Thermotherapy (LITT), *Lasers in Medical Science,19* (2005), 4, PP 197-202.
5. Salavati, M. E., Baygi, M. H. M., A Three-Dimensional Finite Element Model to Study Dynamic Changes of Tissue during Laser Interstitial Thermotherapy, *American Journal of Biomedical Engineering, 5* (2015), 3, pp. 86-93.
6. Chapman, R., New Therapeutic Technique for Treatment of Uterine Leiomyomas Using Laser-Induced Interstitial Thermotherapy (LITT) by a Minimally Invasive Method, Lasers in Surgery and Medicine, 22 (1998), 3, pp. 171-178.
7. Zhang, H., Hua, G., Qian, A., Simulation of Near Infrared Spectroscopy for Laser Induced Interstitial Thermotherapy on Tumors, Applied Mechanics and Materials, 201-202 (2012), pp. 1042-1045.
8. Saccomandi, P., Schena, E., Dimatteo F.M., Pandolfi, M., Martino, M., Rea, R., Silvestri, S., Laser Interstitial Thermotherapy for pancreatic tumor ablation: theoretical model and experimental validation, Conf Proc IEEE, Eng Med Biol Soc., 2011(2011) pp. 55855-8.
9.Tung, M. M., Trujillo, M., Lopez Molina, J. A., Rivera, M. J., Berjano, E. J., Modeling the Heating of Biological Tissue based on the Hyperbolic Heat Transfer Equation, *Elsevier, 50* (2009), 5-6, pp. 665–672.
10.Khalid Salem Shibib, Ayad Zwayen Mohammed, Kholood Hasan Salih, Pulse Laser Parameters Effect on Tissue Thermal Damage Zone in Coagulation Process, Eng.& Tech. Journal,29(2011)5 pp. 972-985.
11.Durkee, J. W., Antich, P. P., Exact solutions to the multi-region time dependent bioheat equation with transient heat sources and boundary conditions, *Physics in Medicine and Biology, 36* (1991), 3, pp. 45-368.
12.Shibib Khalid S.; Minshid Mohammed A.; Tahir Mayada M. Finite element analysis of spot laser of steel welding temperature history, Thermal Science, 13(2009)4, pp. 143-150
13.Welch, A.J., Martin, J.C., *van Gemert, Optical-Thermal Response of Laser Irradiated Tissue Springer Science & Business Media*, Berlin, Germany, 2011.
14.Kannadorai, R. K., Liu, Q., Optimization in interstitial plasmonic photothermal therapy for treatment planning, *Medical Physics, 40* (2013), 10, pp. 1-9.
15.Marqa, M.F., Colin, P., Nevoux, P., Mordon, S., Betrouni, N., Laser Interstitial Thermo Therapy (LITT) for Prostate Cancer Animal Model: Numerical Simulation of Temperature and Damage Distribution, *Proceedings of the COMSOL Conference,* Lasers in Surgery and Medicine, Paris, France,2011, Vol 43.
16.Debatin, J. F., Adam, G., *Interventional Magnetic Resonance Imaging* Springer Science & Business Media, Berlin, Germany, 1998.
17.Peavy,G.M., Lasers and laser–tissue interaction, *The veterinary clinics small animal practice, 32* (2002), pp. 517–534.
18.London, R.A., Glinsky, M.E., Zimmerman, G.B., Bailey, D.S., Eder, D.C., Laser–tissue interaction modeling with LATIS, *Applied Optics,36* (1997), 34, pp. 9068-9074.
19.Mohammed Y. Fattah, Mohammed J. Hamood, Sura Amoori Abbas Simulation of Behavior of Plate on Elastic Foundation under Impact Load by the Finite Element Method, Eng. & Tech. Journal, 31(2013)19 ,pp.44-58.
20.Rao, S. S., The finite element method in engineering, Elsevier Science & Technology Books, Florida, USA, 2004.